https://doi.org/10.5194/wcd-2022-58
Preprint. Discussion started: 18 November 2022

Weather and Climate Dynamics Discussions
Open Access
EGU

Stratospheric influence on the winter North Atlantic storm track in subseasonal reforecasts

Hilla Afargan-Gerstman[1], Dominik Büeler[1], C. Ole Wulff[2], Michael Sprenger[1], and Daniela I.V. Domeisen[3,1]

[1]Institute for Atmospheric and Climate Science, ETH Zurich, Zurich, Switzerland
[2]NORCE Norwegian Research Centre, Bjerknes Centre, Bergen, Norway
[3]University of Lausanne, Lausanne, Switzerland

Correspondence: Hilla Afargan-Gerstman (hilla.gerstman@env.ethz.ch)

Abstract.

Extreme stratospheric polar vortex events, such as sudden stratospheric warmings (SSW) or extremely strong polar vortex (SPV) states, can have a prolonged downward impact influencing surface weather for several weeks to months. SSWs are most often associated with negative North Atlantic Oscillation (NAO) conditions, cold air outbreaks in the Arctic and a southward-shifted extratropical storm track, while SPVs tend to be followed by a positive phase of the NAO, relatively warm conditions in the extratropics and a poleward-shifted storm track. Such changes in the position of the storm track and the associated changes in cyclone frequency over the North Atlantic and Europe can lead to infrastructure damage and health impacts due to cyclone-associated extreme winds and the risk of flooding or heavy snowfall. Skillful predictions of the downward impact of stratospheric polar vortex extremes can therefore improve the predictability of extratropical winter storms on subseasonal timescales. However, there exists a strong inter-event variability in these downward impacts on the tropospheric storm track. Using ECMWF reanalysis data and ECMWF reforecasts from the Subseasonal to Seasonal (S2S) Prediction Project database, we investigate the stratospheric influence on extratropical cyclones, identified with a cyclone detection algorithm. Following SSWs, there is an equatorward shift in cyclone frequency over the North Atlantic in reforecasts, and the opposite response is observed after SPV events, consistent with the response in reanalysis. However, less than 70% of the reforecasts capture the sign of the cyclone frequency response over the North Atlantic during weeks 1-2 after SSWs, and less than 50% of the reforecasts capture the response during weeks 3-4. The cyclone forecasts following SPV events are generally more successful. Understanding the role of the stratosphere in subseasonal variability and predictability of storm tracks during winter can provide a key for reliable forecasts of midlatitude storms and their surface impacts.

1 Introduction

Extratropical cyclones along the North Atlantic storm track have a strong impact on regional weather and climate in Europe, giving rise to extreme weather hazards such as heavy precipitation and strong surface winds. These storms typically develop and intensify over the baroclinic regions in the western part of the North Atlantic, where strong meridional temperature gradients are found. In midlatitudes, the position of the storm track, i.e., the aggregated paths of extratropical cyclones, is closely related

https://doi.org/10.5194/wcd-2022-58
Preprint. Discussion started: 18 November 2022

Weather and Climate Dynamics Discussions
Open Access
EGU

to the jet stream, and is often found on the poleward flank of the jet (e.g., Blackmon et al., 1977; Chang et al., 2002; Shaw et al., 2016). In the North Atlantic, the occurrence of intense extratropical cyclones can produce extreme surface winds, leading in some cases to severe damage over Europe, huge economic losses and even casualties (e.g., Befort et al., 2019). On the other hand, cyclones can strongly influence the evolution of blocking anticyclones downstream (e.g. Pfahl et al., 2015; Steinfeld and Pfahl, 2019), which can lead to cold waves in winter and heat waves in summer (e.g. Kautz et al., 2022). Improving the understanding and prediction of extratropical cyclone activity on subseasonal to seasonal timescales, that is, timescales of several weeks to months, is therefore of great scientific interest and has the potential to provide more accurate forecasts of these storms and reduce the risk of devastating events.

A range of drivers may give rise to increased predication skill on subseasonal to seasonal timescales, including the stratosphere (Baldwin and Dunkerton, 2001; Scaife et al., 2005; Stockdale et al., 2015), tropical variability modes such as the El Niño–Southern Oscillation (ENSO) Brönnimann (2007); Scaife et al. (2014); Domeisen et al. (2015) and the Madden–Julian oscillation (MJO) (Cassou, 2008; Guo et al., 2017; Zheng et al., 2018). These drivers are often associated with external forcing of midlatitude variability acting on longer timescales than the day-to-day weather. Such information is essential for indicating on changes in surface weather several weeks in advance. One of these drivers that can influence storm track behavior in the North Atlantic is the stratosphere, the layer of the Earth's atmosphere between about 10 to 50 km height.

Variability in the stratospheric polar vortex can have a long-lasting influence on surface weather (Baldwin and Dunkerton, 1999, 2001). In particular, a strengthening or weakening of the stratospheric polar vortex can lead to changes in the latitudinal position and strength of the tropospheric jet, associated with the polarity of the NAO, for extended periods of several weeks. Roughly two thirds of extremely weak polar vortex events, known as sudden stratospheric warmings (SSW), are followed by a southward shift of the North Atlantic eddy-driven jet stream (e.g. Karpechko et al., 2017; Maycock et al., 2020a), generally corresponding to a strengthening in the storm track activity over southwestern Europe. For roughly one third of SSW events, the tropospheric response is associated with a poleward shift of the tropospheric jet in the North Atlantic (Afargan-Gerstman and Domeisen, 2020). On the other hand, a strengthening of the stratospheric polar vortex, which can result in so-called strong polar vortex (SPV) events when the stratospheric wind speed increases above a certain threshold, is generally associated with a poleward shift of the North Atlantic jet (Kidston et al., 2015; Goss et al., 2021). In the North Atlantic, such changes in the strength of the stratospheric polar vortex coincide with a latitudinal displacement of the storm track position: weakening of the polar vortex is associated with a southward shift of the storm track, compared with a poleward shift following a strong vortex (Baldwin and Dunkerton, 2001).

The response of the troposphere to stratospheric forcing is generally characterized in terms of changes in the large-scale sea level pressure pattern (Baldwin and Dunkerton, 2001), surface temperature and precipitation patterns (Butler et al., 2017), the NAO (Charlton-Perez et al., 2018; Domeisen, 2019), atmospheric rivers (Lee et al., 2022), or shifts in the eddy-driven jet stream (Maycock et al., 2020b). Less is known about the impact of the stratosphere on the storm track on subseasonal timescales, or how single storms might be affected. However, there are indications that anomalies in the stratospheric polar vortex intensity can provide subseasonal prediction skill for cyclone activity in the eastern Atlantic, Northern Europe and the Iberian Peninsula (Zheng et al., 2019). There exists a range of examples of single storms or series of storms that may have

https://doi.org/10.5194/wcd-2022-58
Preprint. Discussion started: 18 November 2022

Weather and Climate Dynamics Discussions
Open Access
EGU

been driven or at least made more likely by preceding stratospheric events, such as the storms following the 2018 SSW event that triggered the persistent precipitation anomalies ending the Iberian drought (Ayarzagüena et al., 2018) or the storm series that hit the United Kingdom during the record strong Arctic Oscillation in February 2020 that was potentially linked to an extremely strong stratospheric polar vortex (Lawrence et al., 2020; Lee et al., 2020; Rupp et al., 2022). In turn, cyclogenesis can affect the downward impact from the stratosphere (González-Alemán et al., 2022). It is, however, not the goal of this study to attribute single storms to stratospheric origins. In this study, we aim to better characterize the role of the stratosphere in impacting storm tracks and extratropical cyclones.

Here, we evaluate the stratospheric influence on extratropical cyclones in a state-of-the-art Subseasonal to Seasonal (S2S) Prediction model. Cyclone are identified with a cyclone detection algorithm. Cyclone detection schemes for S2S forecasts are not yet common and their use provides a new way of evaluating forecast bias from a weather system perspective. This method is of particular interest following events that may provide windows of opportunity for extending the forecast lead time, as in the case of extreme stratospheric events.

2 Data and Methods

2.1 Reanalysis data and sub-seasonal reforecasts

In order to obtain a better understanding of how the stratosphere affects the storm tracks, we first establish the storm track response in the North Atlantic in reanalysis. We use 24-hourly instantaneous mean sea level pressure (MSLP) from the ERA5 reanalysis (Hersbach et al., 2020) to assess the cyclone frequency for the winter season (December - March) from 2000 to 2019 at a horizontal resolution of $1° \times 1°$ ($\sim$100 km). To identify the lower-tropospheric jet intensity, we use 24-hourly instantaneous 850-hPa zonal wind (U850) obtained from ERA5.

We compare the reanalysis results to a subseasonal prediction system, as this is the relevant tool that will be used to forecast such storms on extended-range timescales. For this purpose, subseasonal reforecasts (also called hindcasts), that is, predictions of past weather, spanning the time period from the 1st of January 2000 until the 31st of December 2019 are used from the ECMWF forecast system. The reforecasts consist of an 11-member ensemble initialized from ERA5 twice a week (on Monday and Thursday) and are run for 46 days. Resolution varies with time, and is approximately 16 km up to day 15, and about 32 km after day 15. These simulations are part of the S2S Prediction research project database, an ongoing research effort for improving the forecast skill and the understanding of the climate system on subseasonal to seasonal timescales (Vitart et al., 2017).

For the major part of this study, in which the spatial characteristics of cyclone frequency are investigated, we use reforecasts from the model cycle 46R1 with 24-hourly instantaneous output. In Section 3.4, which discusses the characteristics of the full cyclone track life cycles, we use 6-hourly output from several model versions with the cycles 47R1, 47R2 and 47R3. A minimum of 6-hourly output is needed for a physically meaningful objective cyclone tracking.

https://doi.org/10.5194/wcd-2022-58
Preprint. Discussion started: 18 November 2022

In this study, we focus on the first four weeks of the reforecasts. For all reforecasts, week 1 is defined as 1-7 days when day 1 is the first day after initialization, week 2 is 8-14 days after initialization, week 3 is at 15-21 days, and week 4 is at 22-28 days.

2.2 Extratropical cyclone identification

Feature-based identification schemes have been developed for cyclones, fronts, warm conveyor belts, and jet streams. In particular, cyclone identification schemes have been widely used for reanalysis data (e.g., Sprenger et al., 2017) as well as for future projections using climate models (Harvey et al., 2020; Priestley and Catto, 2021).

Extratropical cyclones in the ECMWF model are identified from the mean sea level pressure (SLP) field using the Wernli and Schwierz (2006) detection algorithm, refined in Sprenger et al. (2017), as regions delimited by the outermost closed SLP contour enclosing one or several local SLP minima. The position of 6-hourly cyclone tracks are detected according to Sprenger et al. (2017). To neglect weak and short-lived cyclones, we only select the cyclone tracks with a lifetime of at least 24 hours and a maximum intensity (i.e., lowest sea level pressure minimum along the track) of at least 990 hPa.

For every cyclone, the application of the cyclone detection algorithm yields a two-dimensional binary field with a value of 1 at grid points that meet the cyclone criterion and 0 otherwise. The climatology is then computed by temporally averaging the cyclone areas (i.e., the binary fields) (Sprenger et al., 2017). For example, a climatological value of 0.45 in DJF indicates that this grid point is affected by a cyclone 45% of all time steps. We apply this algorithm both on the reanalysis and reforecast data.

Cyclone frequency anomaly for each ensemble member is computed as the difference in the number of cyclones detected in the 28 days after the SSW and the climatological cyclone frequency for this period. Composites of surface impact following stratospheric extreme events are produced by taking the ensemble mean forecast for each of the SSW events as defined below. As the reforecasts are initialized only twice per week, we examine the closest initialization date that occurs either on the same date or after each SSW, hence a date between 0 to 3 days with respect to the SSW central date. For example, for the SSW event on the 12th of February 2018 a reforecast initialized on the 13th of February is used.

2.3 Detection of stratospheric events

For the detection of SSW and SPV events in the reanalysis, we use daily ERA-Interim reanalysis (Dee et al., 2011) for the period 2000–2019. Using ERA-Interim (rather than ERA5) for the identification of stratospheric extreme events allows for a direct comparison of SSW dates with previous work (e.g., Butler et al., 2017). For this modern period used for the model evaluation (2000–2019), the differences in the SSW central dates between ERA-Interim and ERA5 are expected to be minimal and hence do not influence the results of this study.

SSWs are defined as a reversal of the zonal mean zonal winds at 60°N and 10 hPa from westerly to easterly during the extended winter period from November to March, excluding final warming events according to the list given in (Butler and Domeisen, 2021). The central date of the SSW is defined as the first day on which the daily zonal mean zonal winds are easterly. This definition follows Charlton and Polvani (2007) and is commonly used in the literature (Butler et al., 2017). The

https://doi.org/10.5194/wcd-2022-58
Preprint. Discussion started: 18 November 2022

Weather and Climate Dynamics Discussions
Open Access
EGU

winds must return to westerly for at least 20 consecutive days between events, to ensure that each event is counted only once. While Butler et al. (2017) define SSW events for the period 2000–2014, two additional SSW events are included here (12th of February 2018 and 2nd of January 2019), which occurred after the publication of the above study. Overall, 14 SSW events are identified in our study period (2000–2019).

SPV events are defined using a threshold of 48 m s^{-1}. This threshold is the 90th percentile level of the zonal wind at 10 hPa and 60°N from December through March distribution. The central date is the first day of zonal mean zonal winds above this threshold, and the winds must go below 48 m s^{-1} for at least 20 consecutive days between events. Similar thresholds for the detection of SPV events can be found in the literature (e.g., Domeisen et al., 2020b; Oehrlein et al., 2020). Between 2000 and 2019, 14 SPV events are identified according to the above criterion.

3 Results

3.1 Cyclone frequency bias in subseasonal predictions of the ECMWF model

Extratropical cyclone frequencies in the Northern Hemisphere are generally highest over the midlatitude North Pacific and North Atlantic oceans (Hoskins and Hodges, 2002, 2005; Chang et al., 2002; Sprenger et al., 2017). Over the North Atlantic, the highest cyclone frequency occurs between Greenland and Iceland, with a maximum cyclone frequency of 45% (Fig. 1a).

The spatial distribution of cyclone frequency is generally well represented in the reforecasts (Fig. 1b). Yet, the forecast system overestimates the cyclone frequency across midlatitudes between about 40° - 60°N (Fig. 1c), while it underestimates the cyclone frequency along the storm track maximum and south of Greenland.

These results demonstrate the general ability of the ECMWF forecast systems to reproduce the DJFM climatological storm track, although regional biases exist, particularly in the North Atlantic and over Northern Europe, whose origin and consequences will have to be investigated further. A more in-depth analysis of subseasonal reforecast biases for Northern Hemisphere cyclone frequency and life cycle characteristics will be published in a separate future study.

3.2 Zonal wind response following SSW and SPV events

As a next step, we assess the prediction of the surface response following stratospheric extreme events on subseasonal timescales. We first analyze U850 following stratospheric extreme events, focusing on the differences between SSW and SPV events.

Fig. 2 shows a composite of U850 after SSW and SPV events in reforecasts and ERA5 reanalysis. Following SSW events, U850 anomalies in the reforecasts strengthen over the subtropical North Atlantic, particularly equatorward of 40°N, whereas a weakening of the zonal wind occurs between 40° - 60°N in the North Atlantic (Fig. 2a). These changes correspond to an equatorward shift of the eddy-driven jet. Over mid- and high-latitudes of the North Atlantic, as well as over the subtropical Atlantic, U850 anomalies are statistically significant. A similar spatial pattern of the downward impact is found in ERA5 reanalysis, however the maximum weakening occurs further south in the reanalysis compared to the reforecasts, e.g., over the

https://doi.org/10.5194/wcd-2022-58
Preprint. Discussion started: 18 November 2022

Weather and Climate Dynamics Discussions
Open Access
EGU

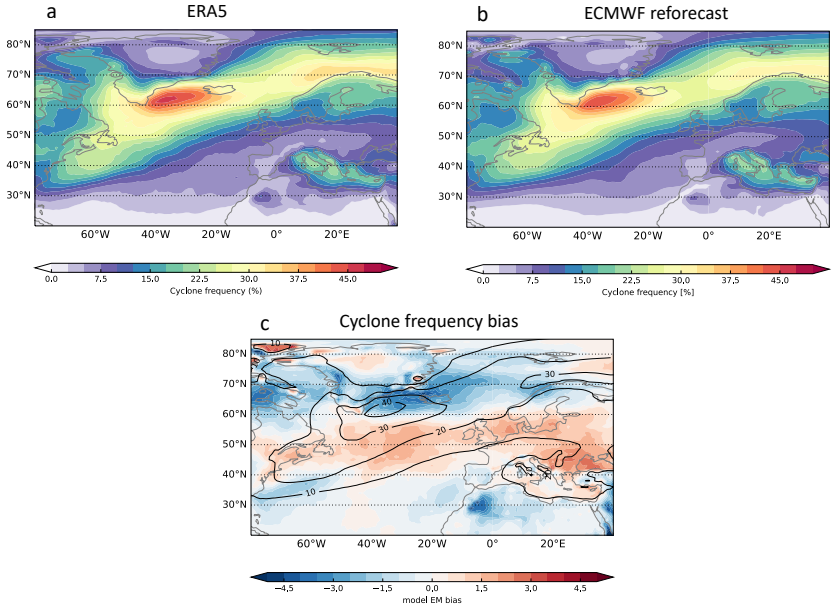

Figure 1. Climatology of cyclone frequency (in %) for December to March (DJFM), in (a) the ERA5 reanalysis for the years 2000-2019, and in (b) the ECMWF reforecasts for the same period. The climatology for the reforecasts is computed using all available initializations between the 1st of December and the 1st of March and averaged over a period of 28 days (days 1-28 with respect to the initialization date). (c) Model bias (shading, in %) according to the difference between ECMWF reforecasts and reanalysis (reforecast minus reanalysis). Black contours in (c) show the climatological cyclone frequency in the reforecasts as shown in panel (b).

North Atlantic as well as over the Baltic Sea and Scandinavia (Fig. 2c). In addition, the response in ERA5 is found to be stronger in ERA5 (Fig. 2c). This is likely related to a few strong individual events that dominate the mean pattern.

In contrast to SSW events, U850 anomalies after SPV events show a strengthening over middle and high latitudes in the North Atlantic in the ECMWF reforecasts, while a weakening of the wind occurs more equatorward, in the subtropical North Atlantic (Fig. 2b). A similar pattern is observed in reanalysis (Fig. 2d). These changes coincide with a poleward jet shift in the North Atlantic region.

3.3 Cyclone frequency response following SSW and SPV events

After SSW events, the North Atlantic storm track in the ECMWF reforecasts strengthens on its southern flank relative to its climatological position and extends further into Europe (Fig. 3a). This response of the North Atlantic storm track is consistent with the change in the North Atlantic jet stream, which also strengthens on its southern flank after SSWs (Fig. 2a). Over Northern Europe, the cyclone frequency response in reanalysis is found to be stronger than in the reforecasts (Fig. 3c).

Consistent with the zonal wind response, cyclone frequency in the SPV composite is enhanced over high latitudes in the North Atlantic (particularly, 60°-70°N) both in the model and in the reanalysis (Fig. 3b,d). The maximum strengthening,

https://doi.org/10.5194/wcd-2022-58
Preprint. Discussion started: 18 November 2022

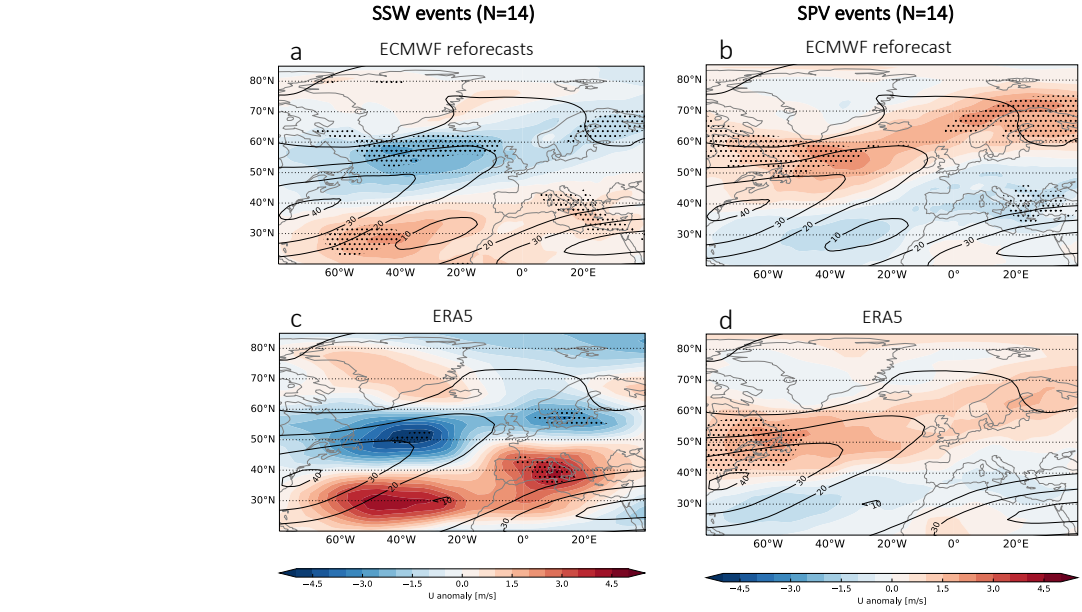

Figure 2. U850 anomalies following (left) sudden stratospheric warming (SSW) and (right) strong polar vortex (SPV) events in (a-b) the ECMWF reforecasts initialized on the same date of the stratospheric extreme events or between 1 to 3 days after their first day, and averaged over a period of 28 days starting on the day of initialization. (c-d) ERA5 reanalysis for the same dates. Black contours show the climatology for DJFM. Anomalies statistically significant at the 95% confidence level based on the Student's t-test are indicated by the hatching.

however, occurs more northeastward in the reanalysis (e.g., over the Norwegian and the Barents Seas, Fig. 3d) compared to the reforecasts, where most of the strengthening is between Greenland and Iceland (Fig. 3b). Both the reanalysis and the reforecasts show a significantly reduced cyclone frequency over the central North Atlantic (particularly, between 30°N to 50°N) (Fig. 3b,d).

Fig. 3e,f shows the difference in cyclone frequency anomalies between reforecasts and reanalysis after SSW (Fig. 3e) and SPV (Fig. 3f) events. After SSWs, the model overestimates cyclone frequency over the central North Atlantic compared to the reanalysis, particularly between 40°N to 50°N and over the Norwegian Sea (Fig. 3e). At higher latitudes, particularly south of Greenland, the reforecasts overestimate the reduction in cyclone frequency after SSW events compared to the reanalysis.

Overestimation of cyclone frequency anomalies in the reforecasts compared to the reanalysis also occurs at higher latitudes (particularly between 60°N to 70°N) after SPV events (Fig. 3f), with statistically significant anomalies along the tilted storm track maximum. Over the central Atlantic the reforecasts underestimate the cyclone frequency relative to the reanalysis.

The regional aspects of the cyclone frequency response after stratospheric extreme events can be more clearly characterized by analyzing the distribution of cyclone frequency anomalies over the central Atlantic after SSW and SPV events. One of the surface impacts of SSW events is the occurrence of anomalously wet conditions over western Europe and the Mediterranean

https://doi.org/10.5194/wcd-2022-58
Preprint. Discussion started: 18 November 2022

and anomalously dry conditions over Scandinavia (e.g., Butler et al., 2017). These changes in precipitation patterns are likely linked to cyclone frequency over these regions. Hence, we here examine whether cyclone frequency after SSW events is indeed increased over the central and southern Atlantic region, and decreased in more poleward regions. For this purpose, we focus our analysis on cyclone frequency in the region between 60°W-0°E, 30°-50°N. This region, located on the southern flank of the North Atlantic storm track, is where the increase in cyclone frequency after SSW events is most intense (black boxes in Fig. 3a,b).

Fig. 4 shows a histogram of cyclone frequency anomalies following SSW and SPV events, compared to all winter days in the reforecasts (grey line). Anomalies are averaged between days 1 to 28 with respect to the central date of the stratospheric event. Over the selected region, the distribution of cyclone frequency anomalies shifts toward positive values after SSW events compared to all winter days (grey curve), both in the reanalysis (grey bins) and the reforecasts (purple) (Fig. 4a). For both of these distributions, however, the shift compared to all winter days is not statistically significant at the 5%-level based on a two-sample Kolmogorov-Smirnov test between two fitted distributions.

In contrast, SPV events are followed by a shift of the distribution toward negative values of cyclone frequency anomalies, relative to all winter days (Fig. 4b). This shift is significant for the reforecasts ($p < 0.02$) but not in the reanalysis. In addition, the distribution of the reforecasts (purple bins) is slightly shifted toward more negative values compared to the reanalysis (grey bins). The statistical significance of this shift in the case of SPV events supports the important role of the stratosphere for the storm track in the North Atlantic, particularly following a strengthened polar vortex. Furthermore, the SPV composite (Fig. 4b) has a narrower distribution compared to the composite of SSW events (Fig. 4a), indicating a broader range of cyclone frequency anomalies following SSW events.

3.4 Cyclone life cycle characteristics following SSW and SPV events

We now investigate how the average cyclone life cycle characteristics depend on the extreme states of the stratospheric polar vortex at forecast initialization. More specifically, we analyze the spatial propagation and intensity characteristics of individual cyclone tracks, which have been identified based on an objective tracking algorithm (see methods for details). Fig. 5 shows all cyclone tracks in the reforecasts and in ERA5 during the 28 days following SSW and SPV events. Independent of the stratospheric state, the highest track densities can be found in the climatological hotspot regions along the U.S. east coast and south of Greenland (cf. black contours in Figs. 5e and 5f, which show the DJFM climatological cyclone frequency), while fewer cyclones are present over Europe and the Mediterranean. Focusing on the median track (blue and red lines, corresponding to SSW and SPV events, respectively), however, reveals a slight equatorward shift of the average cyclone propagation after SSWs, particularly over the eastern half of the North Atlantic and over Europe, which is largely in line with the findings of Baldwin and Dunkerton (2001, see their Fig. 5). However, this shift is only significant (i.e., the two confidence intervals do not overlap; see caption of Fig. 5 for details) in the reforecasts (Fig. 5e) but not in ERA5 (Fig. 5f), which might partly be related to the smaller sample size in ERA5.

We further investigate how extratropical cyclones following SSW and SPV events differ in terms of intensity as an important metric for surface impacts. The cyclones following SPV events tend to reach higher maximum intensities than the cyclones

https://doi.org/10.5194/wcd-2022-58
Preprint. Discussion started: 18 November 2022

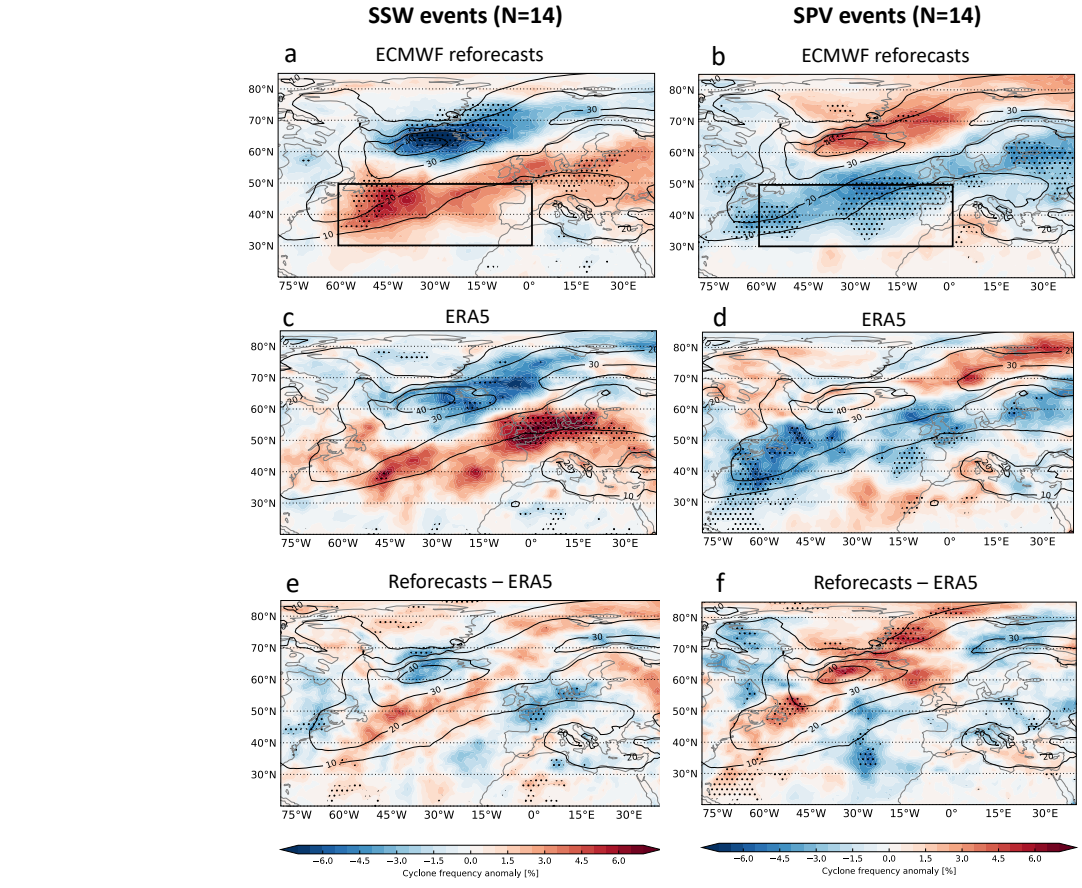

Figure 3. Same as Fig. 2, but for cyclone frequency anomalies (in %). Reforecasts are initialized between 1 to 3 days after the central date of the stratospheric extreme events and averaged over a period of 28 days. ERA5 reanalysis is averaged over the same dates. (e-f) Differences in cyclone frequency anomalies between reforecasts and reanalysis following (e) SSW and (f) SPV events. Black contours show the climatological cyclone frequency in reforecasts for DJFM. Anomalies statistically significant at the 95% confidence level based on the Student's t-test are indicated by the hatching.

following SSW events in both the reforecasts and ERA5, as the shift between the red (SPV) and blue (SSW) distributions in the upper left panels of Figs. 6a and 6b indicates. To determine whether these differences are significant, we split the SSW and SPV distributions into 1%-sized percentile bins, compute the difference between the percentile values of the SSW and SPV distributions for each of these bins (black line in bottom left panels of Figs. 6a and 6b), and check whether this difference is outside the corresponding 99.9% confidence interval (grey shading; see caption of Figs. 6a and 6b for how the confidence interval is computed). According to this analysis, the difference in intensities following SSW and SPV events is

https://doi.org/10.5194/wcd-2022-58
Preprint. Discussion started: 18 November 2022

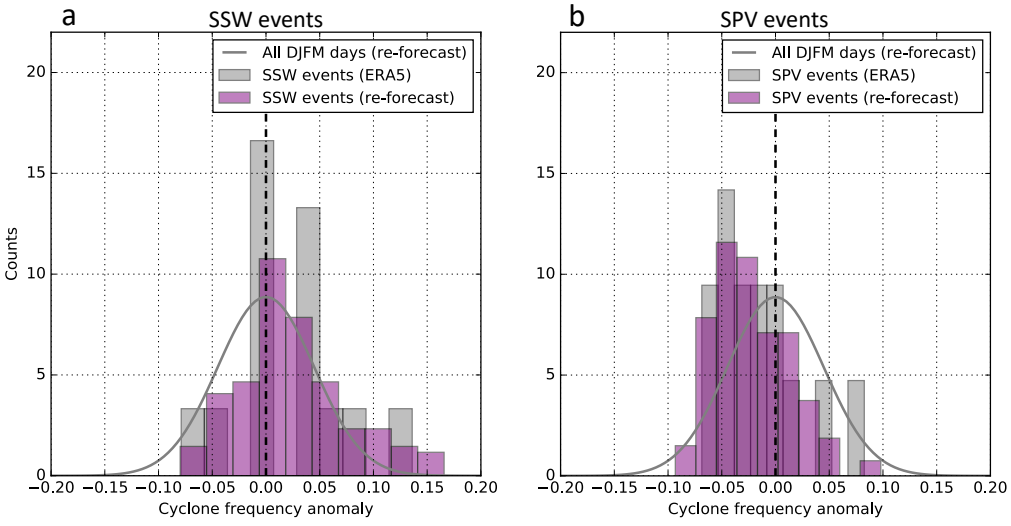

Figure 4. Histogram of cyclone frequency anomalies following (a) SSW and (b) SPV events in the ECMWF reforecasts (purple) and in ERA5 reanalysis (grey) in the North Atlantic (averaged over the black boxes in Fig. 3a,b). Anomalies are averaged over a period of 28 days (days 1-28 with respect to the central date of the stratospheric event). The grey curve indicates the climatological probability density for all days in DJFM in the reforecasts, represented by a normal distribution fitted using the mean and the standard deviation from the original distribution.

highly significant in the reforecasts but only partly significant in ERA5, which, however, might again be related to the smaller sample size in ERA5. To some degree, the higher intensities might be explained by the fact that the more northern cyclones following SPV events (cf. Figs. 5e and 5f) are located in regions with climatologically lower sea level pressure. Nevertheless, the cyclones following SPV events also tend to experience higher maximum intensification rates (upper right panels of Figs. 6a and 6b). The stronger intensification rates might be linked to the larger poleward component of the cyclones' propagation direction as well as the stronger North Atlantic jet following SPV events (cf. Fig. 2), which both correlate with cyclone intensification (e.g., Rivière et al., 2012; Tamarin and Kaspi, 2016; Besson et al., 2021). However, the differences in maximum intensification between SSW and SPV events are not significant in ERA5 and only significant for the most strongly intensifying cyclones (i.e., the lower percentiles) in the reforecasts (bottom right panels of Figs. 6a and 6b).

3.5 Reforecast performance for regional cyclone frequency after SSW and SPV events

Next, the ability of the subseasonal ensemble reforecasts in predicting North Atlantic cyclone frequency after SSW or SPV events is examined (Fig. 7). We focus on the central region of the North Atlantic (60°W-0°E, 30°-50°N, black box in Fig. 3), where anomalous cyclone frequencies are expected following SSW and SPV events (cf. Fig. 3). Red bars in Fig. 7a indicate the proportion of ensemble members that show an average increase in cyclone frequency over this region, whereas blue bars

https://doi.org/10.5194/wcd-2022-58
Preprint. Discussion started: 18 November 2022

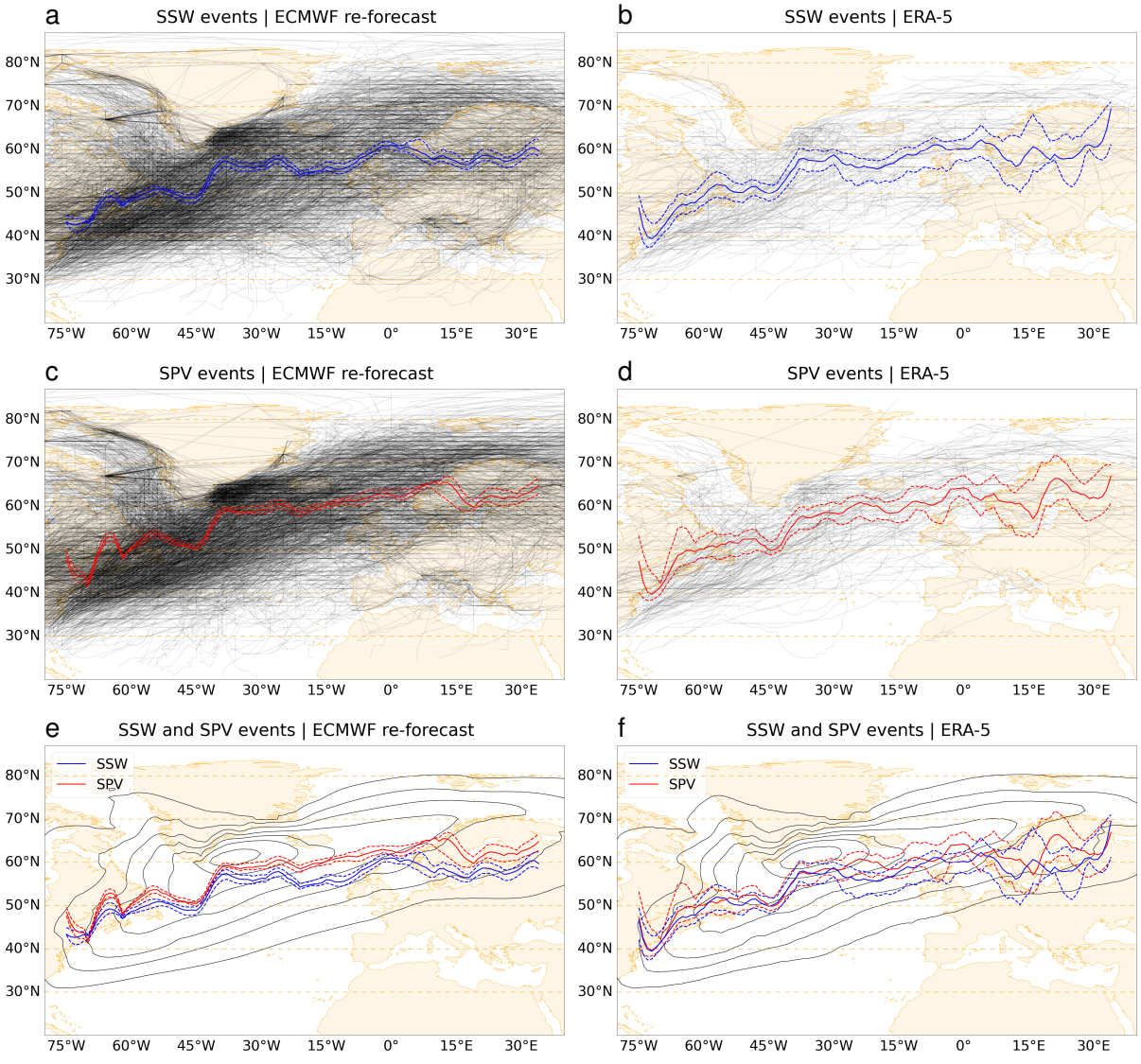

Figure 5. Statistics of individual cyclone tracks with a lifetime of at least 24 hours and a maximum intensity of at least 990 hPa reached within the North Atlantic-European domain in the reforecasts (a, c, e) and in ERA5 (b, d, f). The individual tracks occurring within 28 days after the SSW and SPV events are shown in black (a - d) and the corresponding median latitude (solid) of all tracks in 1-degree longitudinal bands and its 90% confidence interval (dashed) are shown in blue and red. The confidence interval is obtained from a bootstrapped distribution of median latitudes (based on 1000 random resamples of the tracks with replacement). The DJFM cyclone frequency climatology is shown as black contours in (e) and (f).

https://doi.org/10.5194/wcd-2022-58
Preprint. Discussion started: 18 November 2022

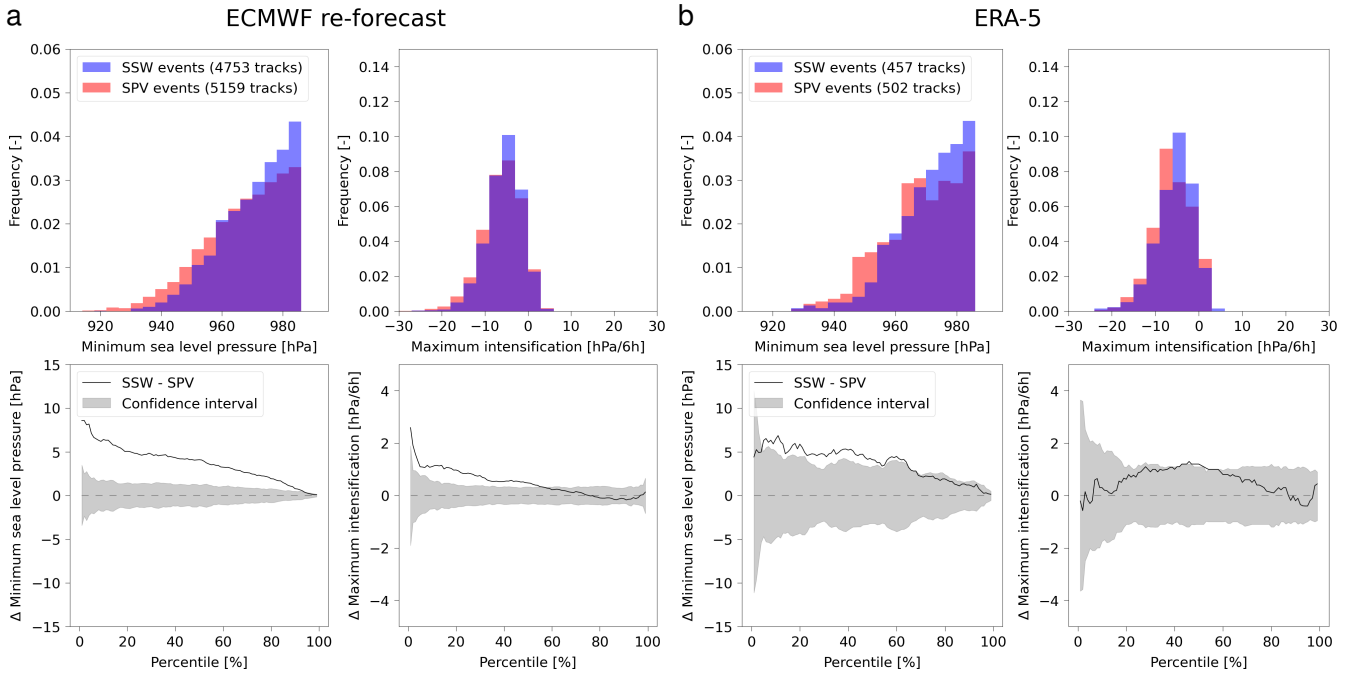

Figure 6. Frequency histograms for maximum intensity (defined as the lowest sea level pressure minimum along the track) and maximum 6-hourly intensification along the track of the cyclones occurring within 28 days after the SSW (blue) and SPV events (red) in the reforecasts and ERA5 are shown in the first row. The corresponding differences between the percentile values of the SSW and SPV distributions are shown by the black lines in the second row (see text for details), complemented by their 99.9% confidence intervals in grey. The confidence intervals are obtained as follows: all data points of both the reforecasts and ERA5 are combined into one distribution and this distribution is randomly shuffled. The shuffled distribution is then split into two new equally sized distributions mimicking the "reforecast" and "ERA5" distributions, and the percentile-wise difference between these two random distributions is computed in the same way as for the original distribution. This procedure is repeated 10000 times to obtain a distribution of differences for each 1%-sized percentile bin.

indicate a decrease. For simplicity, 10 ensemble members (i.e., 10 perturbed simulations of the forecast system, excluding the control run) are analyzed for each event.

The majority of SSW events are followed by an enhancement of cyclone frequency in the central Atlantic in the reanalysis (10 out of 14 events) as indicated by the red stars in Fig. 7. The cyclone frequency response following these events is generally well predicted, with an increase of cyclone frequency identified by more than 60% of the ensemble members in the reforecasts (Fig. 7a). In contrast, the response after SSW events with a decrease in cyclone frequency over the central Atlantic tends to be less predictable, with the majority of ensemble members predicting a decrease in only 1 out of 4 SSW events (Figs. 7a,b).

SPV events, on the other hand, tend to be followed by a decrease in cyclone frequency in the reanalysis (10 out of 14 events). This response is generally well captured by the reforecasts, with 60% or more of the ensemble members predicting the same sign of cyclone frequency anomaly as in the observations in 9 out of 14 events.

https://doi.org/10.5194/wcd-2022-58
Preprint. Discussion started: 18 November 2022

On average over all events, 70% of ensemble members predict a positive sign of the cyclone frequency anomaly in the central Atlantic after SSW events, compared to 30% of ensemble members predicting a negative anomaly. The opposite ratio between ensemble members with an enhanced versus reduced cyclone frequency response is found after SPV events. For SSWs, this ratio corresponds to the percentage of SSW events with a 'canonical' downward response, i.e., an equatorward shift of the North Atlantic jet (e.g., Afargan-Gerstman and Domeisen, 2020).

Another way to evaluate the model performance in predicting anomalies of cyclone frequency is by computing the percentage of hits for SSW and SPV events (Figs. 7b,d). A hit is defined when more than 50% of the ensemble members predict the correct sign (i.e., the same as in reanalysis) of the cyclone frequency anomaly over the selected region.

The ensemble-mean prediction shows that the majority of SSW events with an enhanced cyclone frequency response in the central Atlantic are well predicted (90% of SSWs) in terms of the sign of their downward impact, compared to only 25% of SSW events with a reduced cyclone frequency response (Fig 7b). For comparison, SPV events tend to have higher success rates than SSWs, with more than 75% of SPVs having a successfully predicted cyclone frequency response (Fig. 7d). These success rates are found for SPVs both with an enhanced or reduced response.

Next, we evaluate the hits for each week separately, starting from the central date of the SSW or SPV event (Fig. 8). For the majority of SSW events, the percentage of hits is lower in weeks 3-4 compared to weeks 1-2 (Fig. 8a). Out of 14 SSW events, several events have a low hit rate even in week-1 (e.g., 20 March 2000, 30 December 2001, 24 March 2010). SPV events, on the other hand, are followed by a high hit rate for week-1, with a 100% hit rate for all SPVs except one (11 February 2005; Fig. 8b). The hit rate rapidly drops in the subsequent weeks.

These differences between SSW and SPV events again suggest that the model encounters more difficulties in predicting the cyclone frequency response after SSW events compared to SPV events. The reasons for this behavior can vary between the events: For example, the SSW event of 22 February 2008 was followed by a reduction in cyclone frequency over the central Atlantic (as indicated by the red star in Fig. 7a); while the reforecasts fail to predict the sign of the cyclone frequency response as averaged over a 28-day period after the SSW central date (Fig. 7a), the forecast model prediction for weeks 1 and 2 is in good agreement with observations (Fig. 8a). However, none of ensemble members predicted a positive cyclone frequency response in week-3, and the hit rate remained relatively low in the following week, suggesting that the majority of ensemble members predicted a weakening of the cyclone frequency in the period that followed the SSW.

Overall, this analysis shows that while 70% of the reforecasts capture the sign of the cyclone frequency response over the North Atlantic during weeks 1-2 after SSWs, less than 50% of the reforecasts capture the response during weeks 3-4. The cyclone forecasts following SPV events are generally more successful, with more than 90% of the reforecasts predicting the response during week 1, and around 60% capturing the response in the following weeks.

https://doi.org/10.5194/wcd-2022-58
Preprint. Discussion started: 18 November 2022

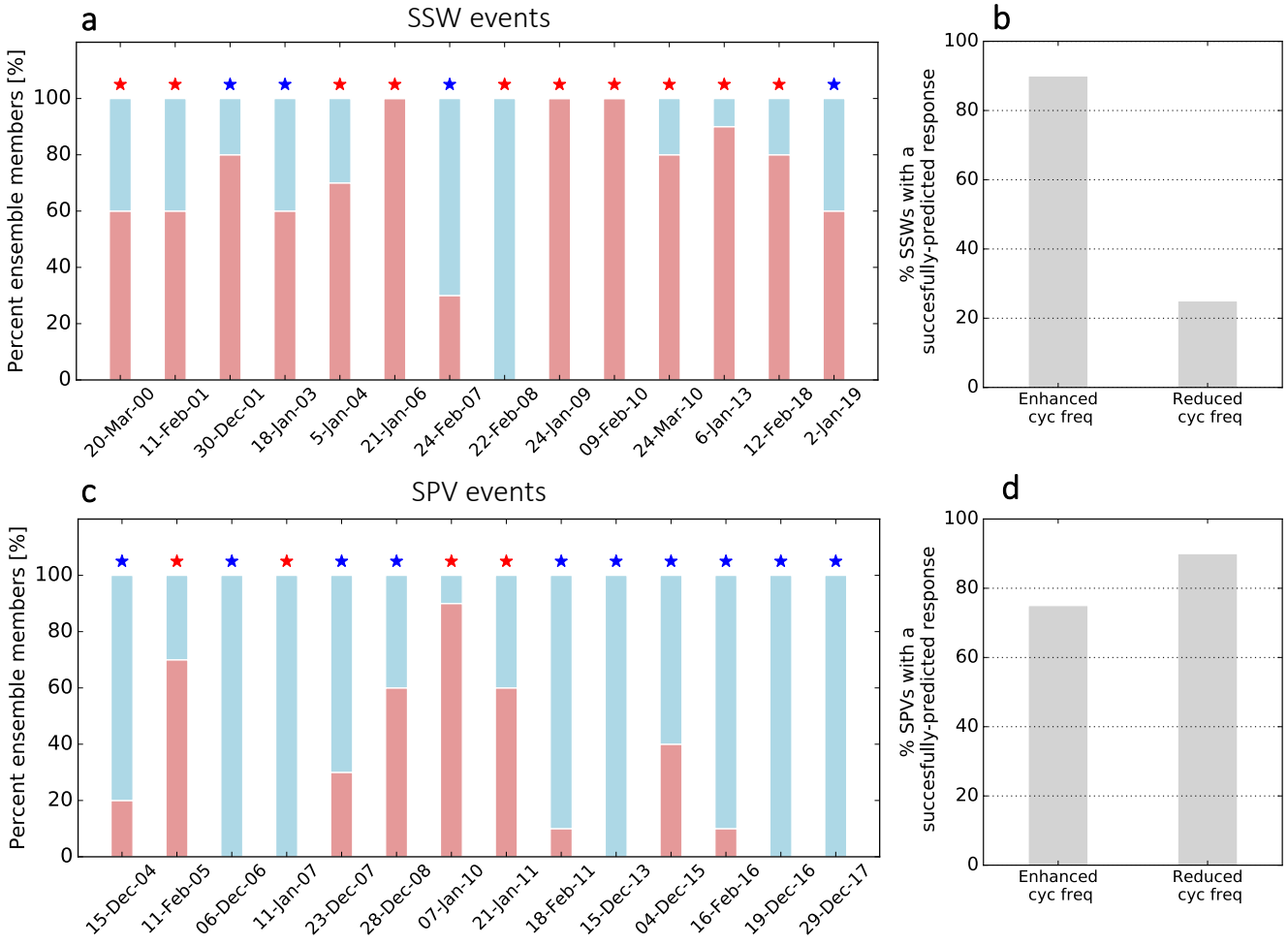

Figure 7. (a,c) Bars represent the percentage of ensemble members that predict an enhancement (red) or a reduction (blue) of cyclone frequency anomaly over the central North Atlantic (black box in Fig. 3a,b) after (a) SSW and (c) SPV events in the ECMWF reforecasts. The x-axis in (a,c) indicates the central dates of the stratospheric events. Anomalies are averaged over days 1-28 of the reforecast. Red and blue asterisks indicate the average response based on ERA5, with red (blue) indicating an increase (decrease) of cyclone frequency anomaly over this region. The percentage of events where more than 50% of the ensemble members predict the correct sign of the cyclone frequency anomaly over the same region for events with enhanced and reduced cyclone frequency, respectively, for (b) SSW and (d) SPV events.

4 Conclusions

Our results show that stratospheric extremes can have a clear impact on the storm track and on cyclone occurrence and tracks, with clear differences between weak and strong stratospheric polar vortex events. In more detail, our results can be summarized as follows:

https://doi.org/10.5194/wcd-2022-58
Preprint. Discussion started: 18 November 2022

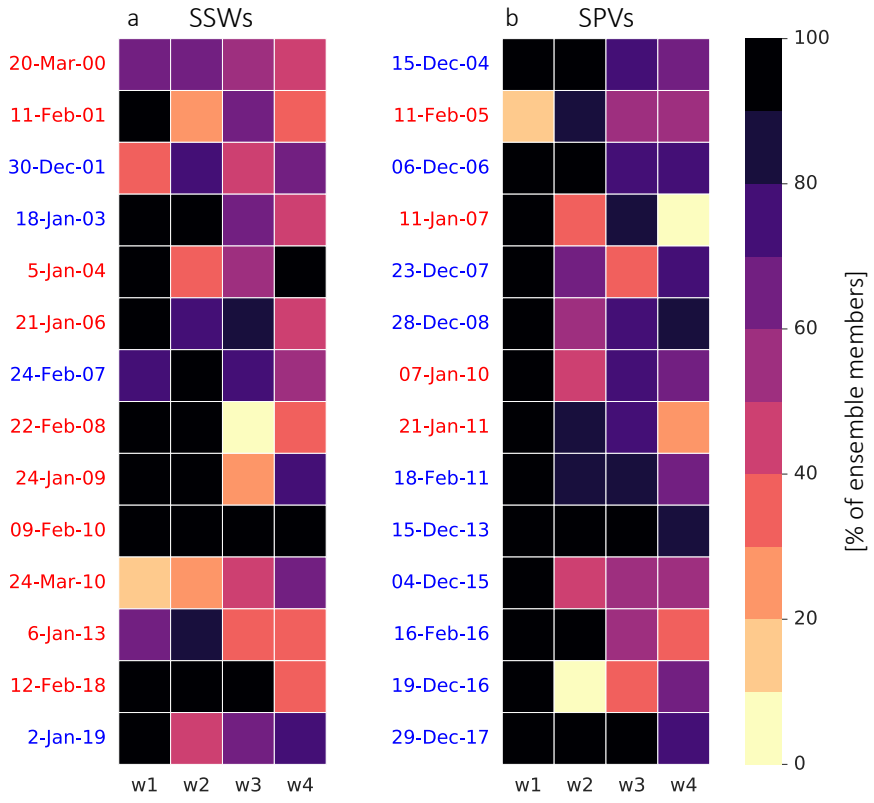

Figure 8. Percentage of ensemble members that successfully predict the observed sign of the cyclone frequency response over the central North Atlantic (60°W-0°E, 30°-50°N) after (a) SSW and (b) SPV events in the ECMWF reforecasts. Anomalies are averaged for every week in the reforecast (w1 is between days 1-7, w2 between days 8-14, etc) with respect to the central date of the event. The observed response is indicted by a red (blue) date corresponding to an increase (decrease) of cyclone frequency anomaly in the selected region.

- The model shows the expected response of the North Atlantic jet stream following stratospheric extreme events (i.e., an equatorward shift after SSW events and a poleward shift after SPV events) when averaging over all events.

- The North Atlantic storm track (measured by the local frequency of cyclone occurrence) exhibits a behavior consistent with the jet, i.e., an enhanced (reduced) cyclone frequency equatorward of the climatological storm track maximum after SSW (SPV) events.

https://doi.org/10.5194/wcd-2022-58
Preprint. Discussion started: 18 November 2022

- The strongest biases in the cyclone frequency model response are observed over northwestern Europe after SSW events, where cyclone frequency is underestimated, and after SPV events to the south and east of Greenland, where cyclone frequency is overestimated.

- The southward shift after SSWs compared to SPV events also manifests itself over the eastern North Atlantic when defining the storm track by the median of individual cyclone tracks. Furthermore, the cyclones after SPV events intensify more strongly and reach higher intensities than after SSW events. However, both the differences in cyclone track location and cyclone intensity are only significant in the reforecasts but not in the reanalysis (with the exception of the significantly stronger cyclone intensities following SPV events also in reanalysis). A larger sample size would be required to determine whether this result is simply due to the smaller sample size in ERA5 or whether this might indicate a slight overconfidence of the reforecasts in predicting the storm track response.

- For individual events, the sign of a canonical (expected) response, i.e., an enhancement (reduction) in cyclone frequency after SSWs (SPVs) in the central North Atlantic is well predicted (in 90% of all cases).

- For SSW and SPV events without a canonical response, the enhanced cyclone frequency in the central North Atlantic after SPV events is well predicted in 75% of all cases, but only in 25% of all cases for SSW events.

- SSWs exhibit significantly more variability between events with respect to predictability. In particular, the surface response to SPV events can almost always be predicted in the first lead week, with a decrease in predictability thereafter, while the predictability behavior for SSW events is much less uniform between events.

Concluding, the model successfully represents the surface cyclone frequency response after most SPV events, especially for short lead times. For SSW events however the results are more mixed: The model is generally more successful in predicting the cyclone frequency after SSWs when the response to the stratospheric events exhibits the canonical response, i.e. an equatorward shift of the storm track. This result points towards a possible overconfidence of the model with respect to reanalysis to predict the canonical response after SSW events, which is however only warranted for about two thirds of SSW events. This result confirms findings for the prediction of the NAO following stratospheric events, which tends to over-predict the occurrence of the negative NAO phase after SSW events (Kolstad et al., 2020, 2022), leading to a poor prediction of surface temperatures over Europe after SSW events (Domeisen et al., 2020a).

These results are consistent with previous studies on the subseasonal prediction of wintertime extratropical cyclones, relating cyclone activity to variations in the stratospheric polar vortex, particularly over the eastern Atlantic, Europe and East Asia (Zheng et al., 2019). We find that the majority of ensemble members predicted a strengthening of the cyclone frequency over the midlatitude Atlantic (60°W-0°E, 30°-50°N) in the period that followed the SSW. These results are in agreement with Rupp et al. (2022).

Further investigation of the role of the stratosphere in subseasonal storm track and cyclone variability will have significant benefits for improving the prediction of extratropical cyclones and large-scale weather patterns in these regions. Understanding of the links between extratropical cyclones and persistent atmospheric circulation patterns, as forced by the downward impact

https://doi.org/10.5194/wcd-2022-58
Preprint. Discussion started: 18 November 2022

of the stratosphere, has the potential to provide more accurate forecasts of intense storm impacts, and helps to reduce the risk against damages incurred by such extreme events.

Code and data availability. The ECMWF reforecast data have been obtained from the ECMWF server at https://apps.ecmwf.int/datasets/data/s2s. The ERA5 reanalysis has been obtained from the ECMWF server (https://www.ecmwf.int/en/forecasts/datasets/reanalysis-datasets/era5, last access: June 2022). ERA-Interim reanalysis has been obtained the ECMWF server (https://apps.ecmwf.int/datasets/data/interim-full-daily/levtype=sfc, last access: June 2022). Cyclone frequency data are available from the corresponding author upon request.

Author contributions. H.A.-G. performed the analysis of the cyclone frequency in the S2S reforecasts, and writing of the manuscript. D.B. performed the analysis of the cyclone life cycle characteristics, and contributed to the writing of the manuscript. C.O.W. provided the S2S reforecasts for the cyclone frequency analysis and contributed to the interpretation of the results. M.S. applied the cyclone detection scheme for the S2S reforecasts and contributed to the interpretation of the results. D.I.V. has contributed to the analysis and interpretation of the results, and to writing of the manuscript. All authors contributed to editing of the final manuscript.

Competing interests. The authors declare that they have no conflict of interest.

Acknowledgements. H.A.-G. acknowledges funding from the European Union's Horizon 2020 research and innovation programme under the Marie Sklodowska-Curie (MSC) (grant agreement No. 891514). Support from the Swiss National Science Foundation through project PP00P2_198896 to D.D. is gratefully acknowledged. D.B. acknowledges funding from the Swiss National Science Foundation (grant no. 205419). C.O.W. acknowledges funding by the Research Council of Norway through the Climate Futures center (Grant 309562).

https://doi.org/10.5194/wcd-2022-58
Preprint. Discussion started: 18 November 2022

Weather and Climate Dynamics Discussions
Open Access
EGU

References

Afargan-Gerstman, H. and Domeisen, D. I. V.: Pacific modulation of the North Atlantic storm track response to sudden stratospheric warming events, Geophysical Research Letters, 47, e2019GL085 007, https://doi.org/10.1029/2019GL085007, 2020.

Ayarzagüena, B., Barriopedro, D., Perez, J. M. G., Abalos, M., de la Camara, A., Herrera, R. G., Calvo, N., and Ordóñez, C.: Stratospheric Connection to the Abrupt End of the 2016/2017 Iberian Drought, Geophysical Research Letters, 45, 12,639–12,646, 2018.

Baldwin, M. P. and Dunkerton, T. J.: Propagation of the Arctic Oscillation from the stratosphere to the troposphere, Journal of Geophysical Research: Atmospheres, 104, 30 937–30 946, 1999.

Baldwin, M. P. and Dunkerton, T. J.: Stratospheric harbingers of anomalous weather regimes, Science, 294, 581–584, 2001.

Befort, D. J., Wild, S., Knight, J. R., Lockwood, J. F., Thornton, H. E., Hermanson, L., Bett, P. E., Weisheimer, A., and Leckebusch, G. C.: Seasonal forecast skill for extratropical cyclones and windstorms, Quarterly Journal of the Royal Meteorological Society, 145, 92–104, 2019.

Besson, P., Fischer, L. J., Schemm, S., and Sprenger, M.: A global analysis of the dry-dynamic forcing during cyclone growth and propagation, Weather and Climate Dynamics, 2, 991–1009, 2021.

Blackmon, M., Wallace, J., Lau, N., and Mullen, S.: An observational study of the Northern Hemisphere wintertime circulation, J. Atmos. Sci., 34, 1040–1053, 1977.

Brönnimann, S.: Impact of El Niño–southern oscillation on European climate, Reviews of Geophysics, 45, 2007.

Butler, A. H. and Domeisen, D. I. V.: The wave geometry of final stratospheric warming events, Weather and Climate Dynamics, 2, 453–474, 2021.

Butler, A. H., Sjoberg, J. P., Seidel, D. J., and Rosenlof, K. H.: A sudden stratospheric warming compendium., Earth System Science Data, 9, 2017.

Cassou, C.: Intraseasonal interaction between the Madden–Julian oscillation and the North Atlantic Oscillation, Nature, 455, 523–527, 2008.

Chang, E. K. M., Lee, S., and Swanson, K. L.: Storm Track Dynamics, J. Climate, 15, 2163–2183, 2002.

Charlton, A. J. and Polvani, L. M.: A new look at stratospheric sudden warmings. Part I: Climatology and modeling benchmarks, Journal of Climate, 20, 449–469, 2007.

Charlton-Perez, A. J., Ferranti, L., and Lee, R. W.: The influence of the stratospheric state on North Atlantic weather regimes, Quarterly Journal of the Royal Meteorological Society, 144, 1140–1151, 2018.

Dee, D. P., Uppala, S. M., Simmons, A. J., Berrisford, P., Poli, P., Kobayashi, S., Andrae, U., Balmaseda, M., Balsamo, G., Bauer, d. P., et al.: The ERA-Interim reanalysis: Configuration and performance of the data assimilation system, Quarterly Journal of the Royal Meteorological Society, 137, 553–597, 2011.

Domeisen, D. I. V.: Estimating the Frequency of Sudden Stratospheric Warming Events from Surface Observations of the North Atlantic Oscillation, Journal of Geophysical Research: Atmospheres, 124, 3180–3194, 2019.

Domeisen, D. I. V., Butler, A. H., Fröhlich, K., Bittner, M., Müller, W. A., and Baehr, J.: Seasonal predictability over Europe arising from El Niño and stratospheric variability in the MPI-ESM seasonal prediction system, Journal of Climate, 28, 256–271, 2015.

Domeisen, D. I. V., Butler, A. H., Charlton-Perez, A. J., Ayarzaguena, B., Baldwin, M. P., Dunn Sigouin, E., Furtado, J. C., Garfinkel, C. I., Hitchcock, P., Karpechko, A. Y., Kim, H., Knight, J., Lang, A. L., Lim, E.-P., Marshall, A., Roff, G., Schwartz, C., Simpson, I. R., Son, S.-W., and Taguchi, M.: The Role of the Stratosphere in Subseasonal to Seasonal Prediction: 2. Predictability Arising From Stratosphere-Troposphere Coupling, Journal of Geophysical Research-Atmospheres, 125, 1–20, 2020a.

https://doi.org/10.5194/wcd-2022-58
Preprint. Discussion started: 18 November 2022

Domeisen, D. I. V., Butler, A. H., Charlton-Perez, A. J., Ayarzagüena, B., Baldwin, M. P., Sigouin, E. D., Furtado, J. C., Garfinkel, C. I., Hitchcock, P., Karpechko, A. Y., Kim, H., Knight, J., Lang, A. L., Lim, E.-P., Marshall, A., Roff, G., Schwartz, C., Simpson, I. R., Son, S.-W., and Taguchi, M.: The role of the stratosphere in subseasonal to seasonal prediction: 2. Predictability arising from stratosphere - troposphere coupling, Journal of Geophysical Research-Atmospheres, https://doi.org/10.1029/2019JD030923, 2020b.

González-Alemán, J. J., Grams, C. M., Ayarzagüena, B., Zurita-Gotor, P., Domeisen, D. I., Gómara, I., Rodríguez-Fonseca, B., and Vitart, F.: Tropospheric role in the predictability of the surface impact of the 2018 sudden stratospheric warming event, Geophysical Research Letters, 49, e2021GL095 464, 2022.

Goss, M., Lindgren, E. A., Sheshadri, A., and Diffenbaugh, N. S.: The Atlantic jet response to stratospheric events: a regime perspective, Journal of Geophysical Research: Atmospheres, 126, e2020JD033 358, 2021.

Guo, Y., Shinoda, T., Lin, J., and Chang, E. K.: Variations of Northern Hemisphere storm track and extratropical cyclone activity associated with the Madden–Julian oscillation, Journal of Climate, 30, 4799–4818, 2017.

Harvey, B., Cook, P., Shaffrey, L., and Schiemann, R.: The response of the northern hemisphere storm tracks and jet streams to climate change in the CMIP3, CMIP5, and CMIP6 climate models, Journal of Geophysical Research: Atmospheres, 125, e2020JD032 701, 2020.

Hersbach, H., Bell, B., Berrisford, P., Hirahara, S., Horányi, A., Muñoz-Sabater, J., Nicolas, J., Peubey, C., Radu, R., Schepers, D., Simmons, A., Soci, C., Abdalla, S., Abellan, X., Balsamo, G., Bechtold, P., Biavati, G., Bidlot, J., Bonavita, M., De Chiara, G., Dahlgren, P., Dee, D., Diamantakis, M., Dragani, R., Flemming, J., Forbes, R., Fuentes, M., Geer, A., Haimberger, L., Healy, S., Hogan, R. J., Hólm, E., Janisková, M., Keeley, S., Laloyaux, P., Lopez, P., Lupu, C., Radnoti, G., de Rosnay, P., Rozum, I., Vamborg, F., Villaume, S., and Thépaut, J.-N.: The ERA5 global reanalysis, Quarterly Journal of the Royal Meteorological Society, 146, 1999–2049, https://doi.org/https://doi.org/10.1002/qj.3803, 2020.

Hoskins, B. J. and Hodges, K. I.: New perspectives on the Northern Hemisphere winter storm tracks, Journal of Atmospheric Sciences, 59, 1041–1061, 2002.

Hoskins, B. J. and Hodges, K. I.: A new perspective on Southern Hemisphere storm tracks, Journal of Climate, 18, 4108–4129, 2005.

Karpechko, A. Y., Hitchcock, P., Peters, D. H., and Schneidereit, A.: Predictability of downward propagation of major sudden stratospheric warmings, Quarterly Journal of the Royal Meteorological Society, 143, 1459–1470, 2017.

Kautz, L.-A., Martius, O., Pfahl, S., Pinto, J. G., Ramos, A. M., Sousa, P. M., and Woollings, T.: Atmospheric blocking and weather extremes over the Euro-Atlantic sector - a review, Weather and Climate Dynamics, 3, 305–336, 2022.

Kidston, J., Scaife, A. A., Hardiman, S. C., Mitchell, D. M., Butchart, N., Baldwin, M. P., and Gray, L. J.: Stratospheric influence on tropospheric jet streams, storm tracks and surface weather, Nature Geoscience, 8, 433, 2015.

Kolstad, E., Lee, S., Butler, A., Domeisen, D., and Wulff, C.: Diverse surface signatures of stratospheric polar vortex anomalies, Journal of Geophysical Research: Atmospheres, p. e2022JD037422, 2022.

Kolstad, E. W., Wulff, C. O., Domeisen, D. I. V., and Woollings, T.: Tracing North Atlantic Oscillation forecast errors to stratospheric origins, Journal of Climate, 33, 9145–9157, 2020.

Lawrence, Z. D., Perlwitz, J., Butler, A. H., Manney, G. L., Newman, P. A., Lee, S. H., and Nash, E. R.: The remarkably strong Arctic stratospheric polar vortex of winter 2020: Links to record-breaking Arctic oscillation and ozone loss, Journal of Geophysical Research: Atmospheres, 125, e2020JD033 271, 2020.

Lee, S. H., Lawrence, Z. D., Butler, A. H., and Karpechko, A. Y.: Seasonal forecasts of the exceptional Northern Hemisphere winter of 2020, Geophysical Research Letters, 47, e2020GL090 328, 2020.

https://doi.org/10.5194/wcd-2022-58
Preprint. Discussion started: 18 November 2022

Lee, S. H., Polvani, L. M., and Guan, B.: Modulation of Atmospheric Rivers by the Arctic Stratospheric Polar Vortex, Geophysical Research Letters, p. e2022GL100381, 2022.

Maycock, A. C., Masukwedza, G. I., Hitchcock, P., and Simpson, I. R.: A regime perspective on the North Atlantic eddy-driven jet response to sudden stratospheric warmings, Journal of Climate, 33, 3901–3917, 2020a.

Maycock, A. C., Masukwedza, G. I. T., Hitchcock, P., and Simpson, I. R.: A Regime Perspective on the North Atlantic Eddy-Driven Jet Response to Sudden Stratospheric Warmings, Journal of Climate, 33, 3901–3917, 2020b.

Oehrlein, J., Chiodo, G., and Polvani, L. M.: The effect of interactive ozone chemistry on weak and strong stratospheric polar vortex events, Atmospheric Chemistry and Physics, 20, 10 531–10 544, 2020.

Pfahl, S., Schwierz, C., Croci-Maspoli, M., Grams, C. M., and Wernli, H.: Importance of latent heat release in ascending air streams for atmospheric blocking, Nature Geoscience, 8, 610–614, 2015.

Priestley, M. and Catto, J.: Changes in cyclone circulation and storm tracks under different future climate scenarios, in: EGU General Assembly Conference Abstracts, pp. EGU21–15 423, 2021.

Rivière, G., Arbogast, P., Lapeyre, G., and Maynard, K.: A potential vorticity perspective on the motion of a mid-latitude winter storm, Geophysical Research Letters, 39, L12 808, 2012.

Rupp, P., Loeffel, S., Garny, H., Chen, X., Pinto, J. G., and Birner, T.: Potential Links Between Tropospheric and Stratospheric Circulation Extremes During Early 2020, Journal of Geophysical Research-Atmospheres, 127, 2022.

Scaife, A., Arribas, A., Blockley, E., Brookshaw, A., Clark, R., Dunstone, N., Eade, R., Fereday, D., Folland, C., Gordon, M., et al.: Skillful long-range prediction of European and North American winters, Geophysical Research Letters, 41, 2514–2519, 2014.

Scaife, A. A., Knight, J. R., Vallis, G. K., and Folland, C. K.: A stratospheric influence on the winter NAO and North Atlantic surface climate, Geophysical Research Letters, 32, 2005.

Shaw, T., Baldwin, M., Barnes, E., Caballero, R., Garfinkel, C., Hwang, Y.-T., Li, C., O'Gorman, P., Rivière, G., Simpson, I., et al.: Storm track processes and the opposing influences of climate change, Nature Geoscience, 2016.

Sprenger, M., Fragkoulidis, G., Binder, H., Croci-Maspoli, M., Graf, P., Grams, C. M., Knippertz, P., Madonna, E., Schemm, S., Škerlak, B., et al.: Global climatologies of Eulerian and Lagrangian flow features based on ERA-Interim, Bulletin of the American Meteorological Society, 98, 1739–1748, 2017.

Steinfeld, D. and Pfahl, S.: The role of latent heating in atmospheric blocking dynamics: a global climatology, Climate Dynamics, 53, 6159–6180, 2019.

Stockdale, T. N., Molteni, F., and Ferranti, L.: Atmospheric initial conditions and the predictability of the Arctic Oscillation, Geophysical Research Letters, 42, 1173–1179, 2015.

Tamarin, T. and Kaspi, Y.: The poleward motion of extratropical cyclones from a potential vorticity tendency analysis, J. Atmos. Sci., 73, 1687–1707, 2016.

Vitart, F., Ardilouze, C., Bonet, A., Brookshaw, A., Chen, M., Codorean, C., Déqué, M., Ferranti, L., Fucile, E., Fuentes, M., et al.: The subseasonal to seasonal (S2S) prediction project database, Bulletin of the American Meteorological Society, 98, 163–173, 2017.

Wernli, H. and Schwierz, C.: Surface cyclones in the ERA-40 dataset (1958–2001). Part I: Novel identification method and global climatology, Journal of the Atmospheric Sciences, 63, 2486–2507, 2006.

Zheng, C., Kar-Man Chang, E., Kim, H.-M., Zhang, M., and Wang, W.: Impacts of the Madden–Julian oscillation on storm-track activity, surface air temperature, and precipitation over North America, Journal of Climate, 31, 6113–6134, 2018.

https://doi.org/10.5194/wcd-2022-58
Preprint. Discussion started: 18 November 2022

Zheng, C., Chang, E. K.-M., Kim, H., Zhang, M., and Wang, W.: Subseasonal to sasonal prediction of wintertime Northern Hemisphere extratropical cyclone activity by S2S and NMME models, Journal of Geophysical Research: Atmospheres, 124, 12,057–12,077, 2019.